Applied and Environmental Microbiology, Aug. 2009, p. 5195–5201 Vol. 75, No. 16
0099-2240/09/$08.00+0 doi:10.1128/AEM.00880-09

Identification of Three Alcohol Dehydrogenase Genes Involved in the Stereospecific Catabolism of Arylglycerol-β-Aryl Ether by *Sphingobium* sp. Strain SYK-6▽†

Yusuke Sato,[1]‡ Hideki Moriuchi,[1]‡ Shojiro Hishiyama,[2] Yuichiro Otsuka,[2] Kenji Oshima,[1] Daisuke Kasai,[1] Masaya Nakamura,[2] Seiji Ohara,[2] Yoshihiro Katayama,[3] Masao Fukuda,[1] and Eiji Masai[1]*

Department of Bioengineering, Nagaoka University of Technology, Nagaoka, Niigata 940-2188,[1] Forestry and Forest Products Research Institute, Tsukuba, Ibaraki 305-8687,[2] and Graduate School of Bio-Applications and Systems Engineering, Tokyo University of Agriculture and Technology, Koganei, Tokyo 184-8588,[3] Japan

Received 18 April 2009/Accepted 11 June 2009

Degradation of arylglycerol-β-aryl ether is the most important process in bacterial lignin catabolism. *Sphingobium* sp. strain SYK-6 degrades guaiacylglycerol-β-guaiacyl ether (GGE) to α-(2-methoxyphenoxy)-β-hydroxypropiovanillone (MPHPV), and then the ether linkage of MPHPV is cleaved to generate α-glutathionyl-β-hydroxypropiovanillone (GS-HPV) and guaiacol. We have characterized three enantioselective glutathione *S*-transferase genes, including two genes that are involved in the ether cleavage of two enantiomers of MPHPV and one gene that is involved in the elimination of glutathione from a GS-HPV enantiomer. However, the first step in the degradation of four different GGE stereoisomers has not been characterized. In this study, three alcohol dehydrogenase genes, *ligL*, *ligN*, and *ligO*, which conferred GGE transformation activity in *Escherichia coli*, were isolated from SYK-6 and characterized, in addition to the previously cloned *ligD* gene. The levels of amino acid sequence identity of the four GGE dehydrogenases, which belong to the short-chain dehydrogenase/reductase family, ranged from 32% to 39%. Each gene was expressed in *E. coli*, and the stereospecificities of the gene products with the four GGE stereoisomers were determined by using chiral high-performance liquid chromatography with recently synthesized authentic enantiopure GGE stereoisomers. LigD and LigO converted (α*R*,β*S*)-GGE and (α*R*,β*R*)-GGE into (β*S*)-MPHPV and (β*R*)-MPHPV, respectively, while LigL and LigN transformed (α*S*,β*R*)-GGE and (α*S*,β*S*)-GGE to (β*R*)-MPHPV and (β*S*)-MPHPV, respectively. Disruption of the genes indicated that *ligD* is essential for the degradation of (α*R*,β*S*)-GGE and (α*R*,β*R*)-GGE and that both *ligL* and *ligN* contribute to the degradation of the two other GGE stereoisomers.

Lignin is a major component of vascular plants and the most abundant aromatic substance in nature. Its degradation by microbes is an essential process in the carbon cycle on Earth. Lignin has various intermolecular linkages between phenylpropane units and contains a number of asymmetric carbons, but it is assumed to be optically inactive (2). Microbes, specifically bacteria, appear to have a variety of stereospecific enzymes which degrade stereoisomers of lignin substructures, but little is known about the stereochemistry of microbial lignin catabolism (10).

Due to the fact that the β-O-4 substructure, arylglycerol-β-aryl ether, is abundant (approximately 50% of the mass) in lignin, the degradation of this structure is considered a crucial step in lignin biodegradation. Arylglycerol-β-aryl ether with two asymmetric carbons in lignin is known to consist of two diastereomers, *erythro* and *threo* isomers. Each diastereomer is thought to be a combination of two enantiomers. In a previous study, we isolated the β-aryl ether catabolic gene cluster, *ligDFEG*, from a degrader of lignin-derived aromatic compounds, *Sphingobium* sp. strain SYK-6 (formerly *Sphingomonas paucimobilis* SYK-6) (8, 11), and these genes code for an alcohol dehydrogenase (12) and three glutathione *S*-transferases (GST) (10). By using racemic preparations of *erythro*-guaiacylglycerol-β-guaiacyl ether (GGE) and α-(2-methoxyphenoxy)-β-hydroxypropiovanillone (MPHPV), we have characterized each gene function of the *ligDFEG* cluster (Fig. 1 and 2). LigD, which belongs to the short-chain dehydrogenase/reductase family (16), initially oxidizes GGE to MPHPV (12), and the ether linkage of MPHPV is cleaved by LigE or LigF; LigE and LigF catalyze glutathione's nucleophilic attack on the carbon atom at the β-position of MPHPV and attack different enantiomers of a racemic MPHPV preparation (10). LigG selectively catalyzes the elimination of glutathione from the resulting α-glutathionyl-β-hydroxypropiovanillone, which is generated by the action of LigF (10). However, all the stereospecific enzymes involved in the oxidation of GGE isomers and the definite stereospecificity of LigD, LigE, and LigF remain unexplained due to the unavailability of the authentic stereoisomers of GGE and MPHPV, whose absolute configurations have been determined previously. Recently, our research group succeeded in chemically synthesizing four enantiopure stereoisomers of GGE and two MPHPV enantiomers (Fig. 1) (S. Hishiyama, Y. Otsuka, M. Nakamura, S. Ohara, E. Masai, and Y. Katayama, submitted for publication). This enabled us to char-

* Corresponding author. Mailing address: Department of Bioengineering, Nagaoka University of Technology, Nagaoka, Niigata 940-2188, Japan. Phone and fax: 81-258-47-9428. E-mail: emasai@vos.nagaokaut.ac.jp.

‡ Y.S. and H.M. equally contributed to this work.

† Supplemental material for this article may be found at http://aem.asm.org/.

▽ Published ahead of print on 19 June 2009.

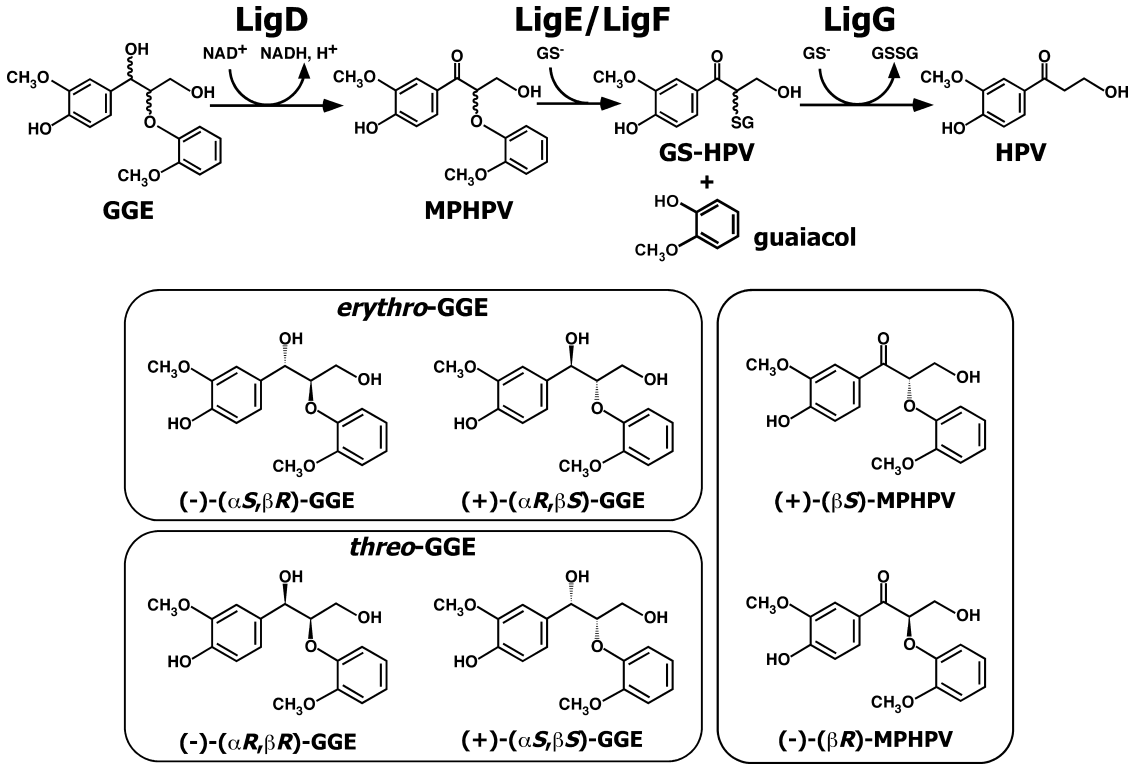

FIG. 1. Catabolic pathway for GGE in *Sphingobium* sp. strain SYK-6. GGE consists of two diastereomers (*erythro* and *threo* isomers), and each diastereomer contains two enantiomers. MPHPV contains two enantiomers. The gene products are as follows: LigD, GGE dehydrogenase (Cα-dehydrogenase); LigE and LigF, GSTs (β-etherase); LigG, GST (glutathione-removing enzyme). Abbreviations: GS^-, reduced glutathione; GSSG, oxidized glutathione; GS-HPV, α-glutathionyl-β-hydroxypropiovanillone; HPV, β-hydroxypropiovanillone.

acterize the genes involved in the stereospecific catabolism of arylglycerol-β-aryl ether.

In this study, we characterized four alcohol dehydrogenase genes, *ligD*, *ligL*, *ligN*, and *ligO*, that confer GGE oxidation activity in *Escherichia coli*. The stereospecificities of the products of these four genes and the contributions of these products to GGE degradation in SYK-6 were determined. This is the first report of enantiomer-based stereochemical characterization of the microbial catabolism of arylglycerol-β-aryl ether.

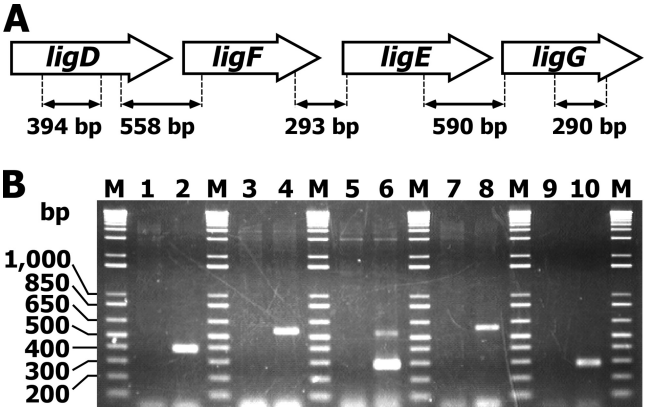

FIG. 2. Operon structure of *ligDFEG* genes. (A) Gene organization for *ligDFEG*. The double-headed arrows under the genetic map indicate the locations of amplified RT-PCR products, whose expected product sizes are indicated. (B) Agarose gel electrophoresis of the RT-PCR products from SYK-6 cells grown in the presence of GGE using primers shown in Table S1 in the supplemental material. The odd-numbered lanes contained controls without reverse transcriptase. Lanes 1 and 2, *ligD* internal region; lanes 3 and 4, *ligD-ligF* intergenic region; lanes 5 and 6, *ligF-ligE* intergenic region; lanes 7 and 8, *ligE-ligG* intergenic region; lanes 9 and 10, *ligG* internal region; lanes M, molecular weight markers.

MATERIALS AND METHODS

Bacterial strains, plasmids, and culture conditions. The bacterial strains and plasmids used in this study are listed in Table 1. *Sphingobium* sp. strain SYK-6 was grown in W minimal salt medium (14) containing 10 mM vanillate or in Luria-Bertani (LB) medium at 30°C. *Sphingomonas sanguinis* IAM 12578 was grown in LB medium. The SYK-6 mutants were grown in LB medium. If necessary, 50 mg of kanamycin/liter, 300 mg carbenicillin/liter, or 12.5 mg of tetracycline/liter was added to the cultures. *E. coli* strains were grown in LB medium at 37°C or 30°C. For cultures of cells carrying antibiotic resistance markers, the media were supplemented with 100 mg of ampicillin/liter, 25 mg of kanamycin/liter, or 12.5 mg of tetracycline/liter.

Chemicals. GGE was purchased from Tokyo Kasei Kogyo Co. (Tokyo, Japan). ^{13}C nuclear magnetic resonance analysis (100 MHz, $CDCl_3$, tetramethylsilane) indicated that GGE from Tokyo Kasei is the *erythro* form (δ values: 87.3 ppm [C-β], 72.4 ppm [C-α], and 61.0 ppm [C-γ]). *threo*-GGE (δ values: 89.4 ppm [C-β], 74.0 ppm [C-α], and 61.0 ppm [C-γ]) was chemically synthesized by the method described by Hosoya et al. (7) and Adler and Eriksoo (1). Enantiopure (+)-(α*R*,β*S*)-GGE ($[\alpha]_D$ = 8.7°), (−)-(α*S*,β*R*)-GGE ($[\alpha]_D$ = −8.5°), (+)-(α*S*,β*S*)-GGE ($[\alpha]_D$ = 43.8°), (−)-(α*R*,β*R*)-GGE ($[\alpha]_D$ = −39.2°), (+)-(β*S*)-MPHPV ($[\alpha]_D$ = 27.9°), and (−)-(β*R*)-MPHPV ($[\alpha]_D$ = −28.5°) prepared in a previous study (Hishiyama et al., submitted for publication) were used as authentic compounds.

RT-PCR. Cells of *Sphingobium* sp. strain SYK-6 were grown in W medium containing 0.2% yeast extract until the optical density at 600 nm of the culture was 0.5. Cells were washed with W medium, transferred to W medium containing 2.5 mM *erythro*-GGE, and incubated for 15 h. Cells were harvested by centrifugation and resuspended in 500 μl of lysis buffer (30 mM Tris-HCl buffer [pH 7.5],

TABLE 1. Strains and plasmids used in this study

Strain or plasmid(s)	Relevant characteristic(s)[a]	Reference or source
Sphingobium sp. strains		
SYK-6	Wild type; Nal^r Sm^r	9
ΔligD	SYK-6 derivative; *ligD*::*kan*; Nal^r Sm^r Km^r	This study
ΔligDL	Δ*ligD* derivative; *ligL*::*bla*; Nal^r Sm^r Km^r Cb^r	This study
ΔligDLN	Δ*ligDL* derivative; *ligN*::*tet*; Nal^r Sm^r Km^r Cb^r Tc^r	This study
S. sanguinis IAM 12578	Nal^r	20
E. coli strains		
HB101	*supE44 hsdS20* (r_B^- m_B^-) *recA13 ara-14 proA2 lacY1 galK2 rpsL20 xyl-5 mtl-1*	3
JM109	*recA1 supE44 endA1 hsdR17 gyrA96 relA1 thi*Δ(*lac-proAB*) F′ (*traD36 proAB*$^+$ *lacI*^{q} *lacZ*ΔM15)	21
BL21(DE3)	F$^-$ *ompT hsdS*$_B$(r_B^- m_B^-) *gal dcm* (DE3); T7 RNA polymerase gene under control of the *lacUV5* promoter	19
Plasmids		
pVK100	Broad-host-range cosmid vector; Km^r Tc^r	5
pRK2013	Tra$^+$ Mob$^+$ ColE1 replicon; Km^r	6
pDH2	pVK100 with partially SalI-digested fragments of SYK-6 carrying *ligL*	This study
pDL1	pVK100 with partially SalI-digested fragments of SYK-6 carrying *ligN*	This study
pDM1	pVK100 with partially SalI-digested fragments of SYK-6 carrying *ligN* and *ligO*	This study
pUC19	Cloning vector; Ap^r	21
pBluescript II KS(+)	Cloning vector; Ap^r	18
pT7Blue	Cloning vector; Ap^r T7 promoter	Novagen
pET21a(+)	Expression vector; Ap^r T7 promoter	Novagen
pIK03	pBluescript II KS(+) with 1.3-kb EcoRV fragment carrying *kan*	13
pKRP12	Tetracycline cassette; Tc^r	15
pK19*mobsacB* and pK18*mobsacB*	*oriT sacB*; Km^r	17
pK19msAp	pK19*mobsacB* with insertion of the 1.0-kb *bla* gene of pUC19 replacing a 0.9-kb BglII-NcoI fragment; Ap^r Cb^r	This study
pUDH30	pUC19 with 3.0-kb SalI fragment carrying *ligD*	12
pTDNE11	pT7Blue with 1.2-kb PCR-amplified fragment carrying *ligD*	This study
pETDa	pET21a(+) carrying 1.1-kb NdeI-EcoRI fragment of pTDNE11	This study
pBDX7	KS(+) with 6.5-kb XhoI fragment carrying *ligL* from pDH2	This study
pTLNE	pT7Blue with 1.0-kb PCR-amplified fragment carrying *ligL*	This study
pETLa	pET21a(+) with 1.0-kb NdeI-SacI fragment of pTLNE	This study
pDL132S	KS(+) with 3.1-kb SalI fragment carrying *ligN* from pDL1	This study
pT7N	pT7Blue with 0.5-kb PCR-amplified fragment carrying part of *ligN*	This study
pETpreNa	pET21a(+) carrying 0.5-kb NdeI-BamHI fragment of pT7N	This study
pETNa	pET21a(+) carrying 2.8-kb NdeI-BamHI fragment carrying *ligN*	This study
pBD345	KS(+) with 4.8-kb EcoRV fragment carrying *ligO* from pDM1	This study
pBDT27	KS(+) with 2.6-kb Tth111I fragment carrying *ligD* from pUDH30	This study
pBDK31	pBDT27 with insertion of *kan* of pIK03 replacing a 0.8-kb StuI-BglII fragment	This study
pKD31K	pK19*mobsacB* with 3.1-kb BamHI-KpnI fragment of pBDK31	This study
pBL25	KS(+) with 2.4-kb EcoRI-SacI fragment carrying *ligL* from pBDX7	This study
pBLAp28	pBL25 with insertion of *bla* of pUC19 replacing a 0.6-kb EcoRV-SalI fragment	This study
pKLAp	pK19msAp carrying 2.8-kb BamHI-XhoI fragment of pBLAp28	This study
pKSN80T	pDL132S with insertion of *tet* from pKRP12	This study
pK18NT	pK18*mobsacB* carrying 5.0-kb SalI fragment of pKSN80T	This study

[a] Nal^r, Sm^r, Km^r, Cb^r, Ap^r, and Tc^r, resistance to nalidixic acid, streptomycin, kanamycin, carbenicillin, ampicillin, and tetracycline, respectively.

100 mM NaCl, 5 mM EDTA, 1% sodium dodecyl sulfate [SDS]). Then a vanadyl ribonucleoside complex was added at a final concentration of 10 mM to the cell suspension, and the suspension was frozen at −80°C. After the cell suspension was thawed, the cells were sonicated, proteinase K was added at a final concentration of 0.2 mg/ml, and the preparation was incubated for 1 h. Following phenol-chloroform-isoamyl alcohol extraction, nucleic acids were precipitated, washed, and resuspended in 100 μl DNase I digestion buffer (20 mM Tris-HCl buffer [pH 8.0], 10 mM $MgCl_2$). Then dithiothreitol, 40 U RNase inhibitor, and 10 U DNase I were added, and the mixture was incubated for 12 h at 37°C. After phenol-chloroform-isoamyl alcohol extraction, nucleic acids were precipitated, washed, and resuspended in 20 μl diethyl pyrocarbonate-treated water containing RNase inhibitor. cDNA was obtained by performing a reverse transcription (RT) reaction using ReverTra Ace (Toyobo, Osaka, Japan) and a hexanucleotide random priming mixture. The cDNA was used as a template for subsequent PCRs with specific primers (see Table S1 in the supplemental material), which amplified the boundaries of *ligD-ligF-ligE-ligG* (accession no. D11473 and AB026292). Control samples from which reverse transcriptase was omitted were used in parallel RT-PCRs.

Cloning of *ligL*, *ligN*, and *ligO*. A partially SalI-digested gene library of SYK-6 constructed with pVK100 as the vector was introduced into the host strain *S. sanguinis* IAM 12578 by triparental mating (5). The ability of 1,700 transconjugant cells to oxidize *erythro*-GGE was monitored by determining the increase in absorbance at 356 nm derived from the carbonyl group of MPHPV (ε_{356} = 39,000 $M^{-1}cm^{-1}$; pH 8.5) with a DU-7500 spectrophotometer (Beckman Coulter, Inc., Fullerton, CA). Eight cosmid clones were isolated, and seven cosmids were selected as clones that conferred oxidation activity with GGE, which was prepared by incubation of *erythro*-GGE with cell extract of *E. coli* BL21(DE3) harboring pETDa carrying *ligD*. Southern hybridization analysis of cosmid clones with each cosmid clone digested with SalI as a probe was carried out using the digoxigenin (DIG) system (Roche Diagnostics, Indianapolis, IN).

Subcloning was performed to clone the 6.5-kb XhoI fragment carrying *ligL* from pDH2, the 3.1-kb SalI fragment carrying *ligN* from pDL1, and the 4.8-kb EcoRV fragment carrying *ligO* from pDM1 into pBluescript II KS(+). The nucleotide sequences of these fragments were determined by the dideoxy termination method with a CEQ 2000XL genetic analysis system (Beckman Coulter). Sequence analysis was performed with the GeneWorks program (Intelligenetics, Inc., Mountain View, CA) and MacVector (MacVector, Inc., Cary, NC). Homology searches were performed with the nonredundant protein sequence database by using the BLASTP program. Pairwise alignment was performed with the EMBOSS alignment tool at the homepage of the European Bioinformatics Institute (http://www.ebi.ac.uk/emboss/align).

Expression of *ligD*, *ligL*, *ligN*, and *ligO* in *E. coli*. Construction of pETDa, pETLa, pETNa, and pBD345 for expression of *ligD*, *ligL*, *ligN*, and *ligO*, respectively, is described in the supplemental material. pETDa, pETLa, and pETNa were introduced into *E. coli* BL21(DE3) cells, and pBD345 was introduced into *E. coli* JM109 cells. The *E. coli* transformants were grown in LB medium containing 100 mg ampicillin/liter at 30°C. Expression of the genes was induced for 4 h by adding 1 mM isopropyl-β-D-thiogalactopyranoside when the optical density at 600 nm of the culture reached 0.5. Cells were harvested by centrifugation and suspended in 50 mM Tris-HCl buffer (pH 8.5). The cells suspended in the buffer were sonicated, and the cell lysate was centrifuged at 15,000 × *g* for 10 min. The resulting supernatant was used as the cell extract. Protein concentrations were determined using the Bradford method (4). Expression of the genes was confirmed using SDS-12% polyacrylamide gel electrophoresis (PAGE). Gels were stained with Coomassie brilliant blue.

Construction of mutants. Construction of a *ligD* mutant (ΔligD), a *ligD ligL* double mutant (ΔligDL), and a *ligD ligL ligN* triple mutant (ΔligDLN) is described in the supplemental material. To examine the disruption in each gene, Southern hybridization analysis was performed. Total DNA of candidates for ΔligD, ΔligDL, and ΔligDLN were digested with ApaI, EcoRI-SacI, and SalI, respectively. A 1.8-kb ApaI fragment carrying *ligD*, a 1.1-kb SacII-Eco47III fragment carrying *ligL*, a 0.7-kb StuI-EcoRI fragment carrying *ligN*, a 1.3-kb EcoRV fragment carrying *kan*, and a 1.0-kb BspHI fragment carrying *bla* were labeled with the DIG system and used as probes (see Fig. S1 in the supplemental material).

Determination of the stereospecificities of GGE dehydrogenases. Cell extracts of *E. coli* transformants (500 μg of protein) were incubated with 1 mM *erythro*-GGE or *threo*-GGE in the presence of 10 mM NAD^+ in a 1-ml reaction mixture containing 50 mM Tris-HCl buffer (pH 8.5) at 30°C for 12 h. The reaction mixture was acidified with hydrochloric acid, extracted with ethyl acetate, and separated repeatedly by thin-layer chromatography using Silica Gel 60 F254 (E. Merck, Darmstadt, Germany). The developing solvent was chloroform-methanol (95:5 [vol/vol]). Compounds were visualized under UV light at 254 nm, and an upper spot and a lower spot corresponding to MPHPV and GGE were cut out, extracted with ethyl acetate, and finally dissolved in tetrahydrofuran. Compounds were analyzed by using a high-performance liquid chromatography (HPLC) system (Alliance 2690 separation module; Waters, Milford, Mass.) equipped with a Chiralcel OD-H column (4.6 by 250 mm; Daicel Chemical Industries, Tokyo, Japan). The mobile phase was a mixture of hexane (89.5%), ethanol (9.5%), and acetic acid (1%), and the flow rate was 0.5 ml/min. The column temperature was maintained at 30°C. GGE and MPHPV were detected at 280 and 310 nm, respectively.

Characterization of mutants. SYK-6, ΔligD, ΔligDL, and ΔligDLN were grown in LB medium until the optical density at 600 nm of the culture was 0.5. The method used for preparation of cell extracts was the same as the method described above. Cell extracts (1 mg of protein/ml) were incubated with 50 μM *erythro*-GGE and *threo*-GGE in a reaction mixture containing 50 mM Tris-HCl (pH 8.5) and 500 μM NAD^+ at 30°C. Degradation of GGE was periodically analyzed with an Alliance 2690 separation module HPLC system equipped with a Tskgel ODS-80 column (6 by 150 mm; Tosoh, Tokyo, Japan). The mobile phase was a mixture of water (49.5%), acetonitrile (49.5%), and phosphoric acid (1%), and the flow rate was 1 ml/min. GGE and MPHPV were detected at 280 and 310 nm, respectively. The retention times of GGE and MPHPV were 4.1 and 4.9 min, respectively.

Nucleotide sequence accession numbers. The nucleotide sequences reported in this paper have been deposited in the DDBJ, EMBL, and GenBank nucleotide sequence databases under accession no. AB491221, AB491222, and AB491223.

RESULTS AND DISCUSSION

RT-PCR analysis of the *ligDFEG* gene cluster. To determine the operon structure of the *ligDFEG* genes, which encode an alcohol dehydrogenase and three GSTs involved in the cleavage of arylglycerol-β-aryl ether, RT-PCR analysis was performed with total RNA isolated from SYK-6 cells grown in the presence of 2.5 mM *erythro*-GGE and primers complementary to neighboring genes. Amplification products were obtained for *ligD-ligF* (558 bp), *ligF-ligE* (293 bp), and *ligE-ligG* (590 bp) (Fig. 2). These results indicated that together, the *ligDFEG* genes constitute an operon for catabolism of arylglycerol-β-aryl ether.

Stereospecificity of LigD for GGE stereoisomers. Based on comparison with authentic GGE stereoisomers, we separated *erythro*-GGE into (α*S*,β*R*)-GGE and (α*R*,β*S*)-GGE fractions with retention times of 41.6 and 44.6 min, respectively, on a chiral column by HPLC (Fig. 3A), and we separated *threo*-GGE into (α*R*,β*R*)-GGE and (α*S*,β*S*)-GGE fractions with retention times of 44.3 and 47.7 min (Fig. 3C). On the other hand, racemic MPHPV was separated into (β*S*)-MPHPV and (β*R*)-MPHPV fractions with retention times of 41.6 and 52.5 min, respectively (Fig. 3B and D).

The *ligD* gene was cloned in pET21a(+) to generate pETDa, and *ligD* was expressed in *E. coli* BL21(DE3) harboring pETDa. SDS-PAGE showed that a 31-kDa protein was produced in the *E. coli* transformant, and this size was in good agreement with the value calculated from the amino acid sequence deduced for *ligD* (M_r, 32,341). The cell extract of *E. coli* BL21(DE3) harboring pETDa (500 μg of protein/ml) was incubated with 1 mM *erythro*-GGE and *threo*-GGE in the presence of NAD^+ for 12 h at 30°C. Compounds in the reaction mixture were extracted with ethyl acetate and subjected to thin-layer chromatography to separate the substrate (GGE) from the product (MPHPV). The separated compounds were analyzed by chiral HPLC. This analysis revealed the disappearance of (α*R*,β*S*)-GGE and the generation of (β*S*)-MPHPV from *erythro*-GGE (Fig. 3E and F), as well as the disappearance of (α*R*,β*R*)-GGE and the generation of (β*R*)-MPHPV from *threo*-GGE (Fig. 3G and H). These results clearly indicated that LigD converted (α*R*,β*S*)-GGE and (α*R*,β*R*)-GGE into (β*S*)-MPHPV and (β*R*)-MPHPV, respectively. These results also suggested that other GGE dehydrogenases are involved in the oxidation of (α*S*,β*R*)-GGE and (α*S*,β*S*)-GGE.

Role of *ligD* in the catabolism of arylglycerol-β-aryl ether. In order to estimate whether LigD actually plays a role in the degradation of (α*R*,β*S*)-GGE and (α*R*,β*R*)-GGE, the *ligD* gene in SYK-6 was disrupted by using the gene replacement technique with the *ligD* disruption plasmid pKD31K, which was constructed by replacing the 0.8-kb StuI-BglII fragment of *ligD* in pK19*mobsacB* with the *kan* gene (see Fig. S1 in the supplemental material). An extract of SYK-6 cells (1 mg of protein/ml) grown in W medium containing vanillate was able to transform almost all the 50 μM *erythro*-GGE and *threo*-GGE during 3 h of incubation in the presence of NAD^+ (Fig. 4). On the other hand, a cell extract (1 mg of protein/ml) of the *ligD* mutant, ΔligD, transformed only 50% of both *erythro*-GGE and *threo*-GGE. However, the initial rates of GGE degradation for ΔligD and the wild type were almost the same (Fig. 4). These results strongly suggested that *ligD* is essential for the conversion of (α*R*,β*S*)-GGE and (α*R*,β*R*)-GGE.

Cloning of alternative GGE dehydrogenase genes. A cosmid library of SYK-6 constructed in *S. sanguinis* IAM 12578, which has no GGE transformation activity, was screened for clones

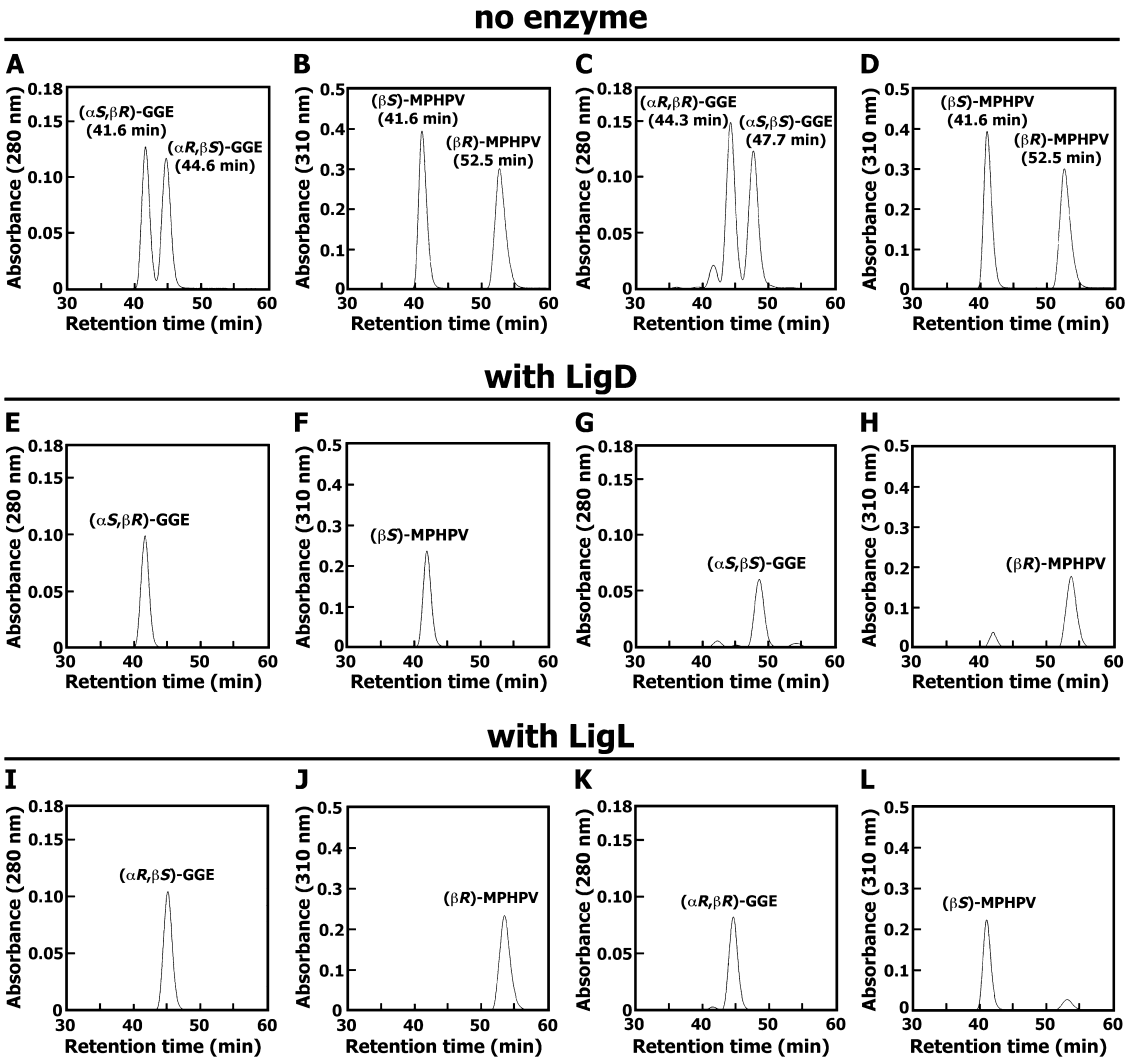

FIG. 3. Stereospecificities of LigD and LigL for GGE stereoisomers. (A and C) Chiral HPLC profiles of authentic *erythro*-GGE and *threo*-GGE, respectively. (B and D) Chiral HPLC profiles of authentic racemic MPHPV. (E to L) Crude LigD (E to H) and LigL (I to L) were incubated with 1 mM *erythro*-GGE and *threo*-GGE. (E and F) Chiral HPLC profiles of unreacted GGE and MPHPV produced from *erythro*-GGE in the reaction catalyzed by LigD, respectively. (G and H) Chiral HPLC profiles of unreacted GGE and MPHPV produced from *threo*-GGE in the reaction catalyzed by LigD, respectively. (I and J) Chiral HPLC profiles of unreacted GGE and MPHPV produced from *erythro*-GGE in the reaction catalyzed by LigL, respectively. (K and L) Chiral HPLC profiles of unreacted GGE and MPHPV produced from *threo*-GGE in the reaction catalyzed by LigL, respectively.

capable of oxidizing *erythro*-GGE. Of the 1,700 clones tested, 7 showed oxidation activity with (α*S*,β*R*)-GGE prepared from *erythro*-GGE by incubation with crude LigD enzyme. Southern hybridization analysis of the cosmid clones using each SalI-digested cosmid as a probe suggested that these clones could be categorized into three types of cosmids, pDH2, pDM1, and pDL1 (data not shown). Both pDM1 and pDL1 included the same 3.1-kb SalI fragment, but other SalI fragments were different from each other. Since the *ligD* probe hybridized to the 6.5-kb XhoI fragment of pDH2 at low stringency, the nucleotide sequence of this fragment was determined. The 4.3-kb XhoI-SalI fragment included in the 6.5-kb XhoI fragment contained three open reading frames (ORFs), and the deduced amino acid sequence encoded by the 867-bp ORF showed 36% identity with the deduced amino acid sequence encoded by *ligD*. This ORF, designated *ligL*, was located between a 543-bp ORF encoding a staphylococcal nuclease homologue superfamily protein (conserved domain accession no. cl00140) and a 1,221-bp ORF which encoded a putative threonine synthase. The common 3.1-kb SalI fragment of pDM1 and pDL1 was cloned from pDL1 in pBluescript II KS(+) to generate pDL132S. *E. coli* JM109 harboring pDL132S exhibited *erythro*-GGE oxidation activity. Analysis of the nucleotide sequence of the 3.1-kb SalI fragment revealed the presence of a 933-bp ORF which showed 32% identity with LigD at the amino acid sequence level, and this ORF was designated *ligN*. A 984-bp ORF, which encoded a putative oxidoreductase, was found downstream of *ligN*. In addition, the 4.8-kb EcoRV fragment of pDM1 conferred *erythro*-GGE oxidation activity in *E. coli* JM109. This fragment was found to contain an 891-bp ORF whose product exhibited 39% identity with LigD at the amino acid sequence level. This ORF was designated *ligO*. Down-

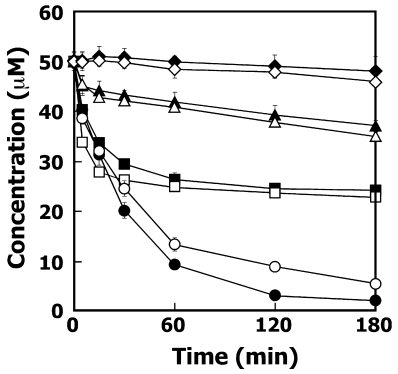

FIG. 4. Conversion of *erythro*-GGE and *threo*-GGE by SYK-6, ΔligD, ΔligDL, and ΔligDLN. Conversion of 50 μM *erythro*-GGE and *threo*-GGE by cell extracts (1 mg of protein/ml) of SYK-6 (circles), ΔligD (squares), ΔligDL (triangles), and ΔligDLN (diamonds) in the presence of NAD^+ was periodically monitored by HPLC. Filled symbols, *erythro*-GGE; open symbols, *threo*-GGE. The data are the averages ± standard deviations (error bars) of at least three measurements.

stream of *ligO*, 546-bp and 1,548-bp ORFs were found, but their functions were not predicted based on sequence similarity. The levels of amino acid sequence identity between LigD, LigL, LigN, and LigO ranged from 32% to 39%. A BLASTP search demonstrated that putative short-chain dehydrogenases/reductases encoded by YP_495487, YP_497149, and YP_496073 of *Novosphingobium aromaticivorans* DSM 12444 were most similar to LigD (77% identity; expected value [e value], $2e^{-122}$), LigL (48% identity; e value, $4e^{-68}$), and LigN (44% identity; e value, $6e^{-57}$), respectively. The amino acid sequence encoded by *ligO* is most similar to the sequences encoded by *ligD* (41% identity; e value, $2e^{-59}$) and YP_496072 (41% identity; e value, $5e^{-57}$) of DSM 12444. These results suggested that DSM 12444 might also possess multiple GGE dehydrogenase genes. Interestingly, YP_496073 is an upstream neighbor of YP_496072 in the DSM 12444 genome. This fact corresponds to the fact that *ligN* and *ligO* are located in the same cosmid, pDM1; however, the precise location of these two genes in SYK-6 was not studied here.

Stereospecificities of LigL, LigN, and LigO for GGE stereoisomers. The *ligL* and *ligN* genes cloned in pET21a(+) were expressed in *E. coli* BL21(DE3), and SDS-PAGE revealed production of 33-kDa proteins in both cell extracts. This size was in good agreement with the values calculated from the deduced amino acid sequences encoded by *ligL* (M_r, 31,298) and *ligN* (M_r, 32,924). On the other hand, *ligO* in pBD345 was expressed in *E. coli* JM109, but SDS-PAGE did not show the gene product. The weak expression of *ligO* in *E. coli* was probably due to the GTG start codon of *ligO*. Since the oxidation activity with *erythro*-GGE was present in the cell extract of *E. coli* harboring pBD345, the crude LigO enzyme was used in the following analysis. The cell extract of each transformant (500 μg of protein/ml) was incubated with 1 mM *erythro*-GGE

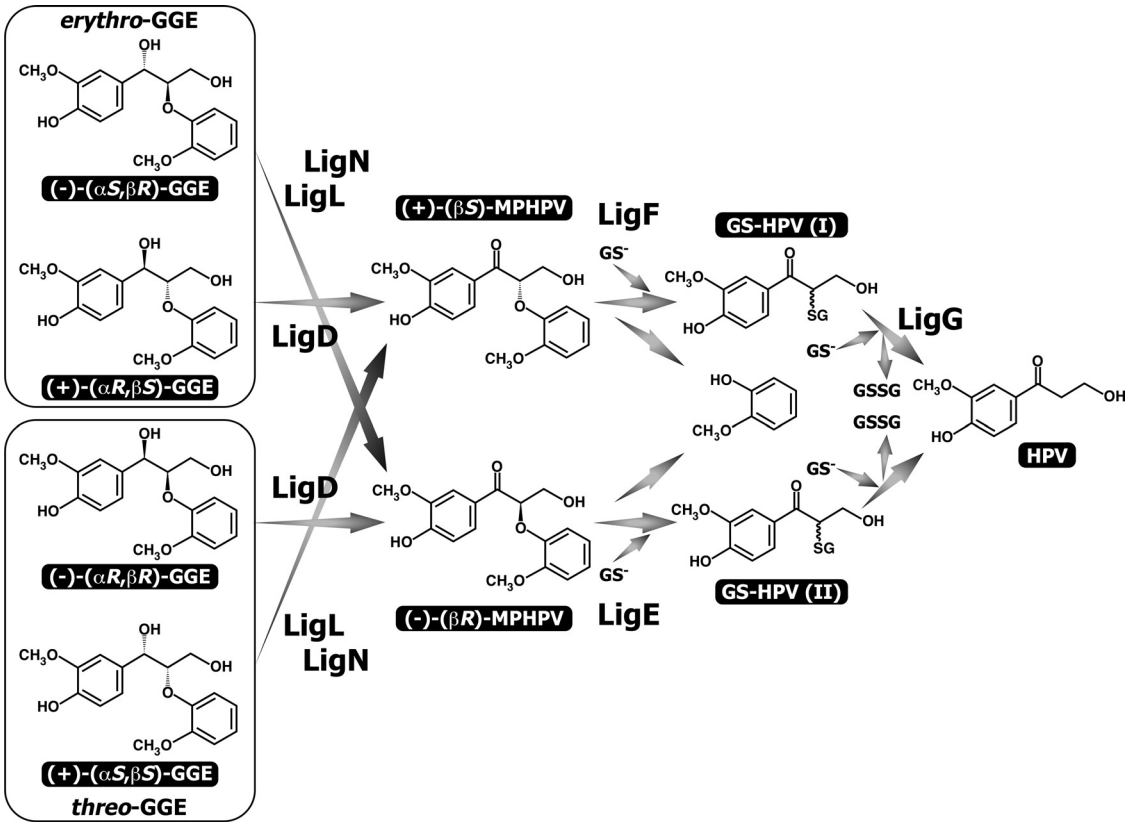

FIG. 5. Catabolic pathway for GGE stereoisomers in *Sphingobium* sp. strain SYK-6. Abbreviations: GS^-, reduced glutathione; GSSG, oxidized glutathione; GS-HPV, α-glutathionyl-β-hydroxypropiovanillone; HPV, β-hydroxypropiovanillone.

and *threo*-GGE in the presence of NAD^+ to determine their stereospecificities. Chiral HPLC analysis indicated that LigL and LigN have the same stereospecificity and transformed (α*S*,β*R*)-GGE and (α*S*,β*S*)-GGE to (β*R*)-MPHPV and (β*S*)-MPHPV, respectively (Fig. 3; see Fig. S2 in the supplemental material). On the other hand, LigO converted (α*R*,β*S*)-GGE and (α*R*,β*R*)-GGE into (β*S*)-MPHPV and (β*R*)-MPHPV, respectively (see Fig. S3 in the supplemental material). These results indicated that LigO has the same stereospecificity as LigD. However, *ligO*'s contribution to the degradation of (α*R*,β*S*)-GGE and (α*R*,β*R*)-GGE appeared to be negligible, because ΔligD did not degrade 50% of *erythro*-GGE and *threo*-GGE (Fig. 4).

Role of *ligL* and *ligN* in the catabolism of arylglycerol-β-aryl ether. The *ligL* gene in ΔligD was disrupted by homologous recombination between *ligL* in ΔligD and the disrupted *ligL* gene by replacing the 0.6-kb EcoRV-SalI fragment in the structural gene of *ligL* with the *bla* gene in pKLAp, as shown in Fig. S1 in the supplemental material. The rate of conversion of 50 μM *erythro*-GGE and *threo*-GGE in the presence of NAD^+ by the cell extract (1 mg of protein/ml) of the *ligD ligL* double mutant, ΔligDL, decreased remarkably, but this mutant degraded approximately 20% of the substrate (Fig. 4). Therefore, we constructed the *ligD ligL ligN* triple mutant by introducing *ligN* disruption plasmid pK18NT into ΔligDL cells. The triple mutant, ΔligDLN, was obtained by homologous recombination between *ligN* and the inactivated *ligN* by insertion of the *tet* gene, as shown in Fig. S1 in the supplemental material. An extract of ΔligDLN cells (1 mg of protein/ml) was incubated with 50 μM *erythro*-GGE and *threo*-GGE in the presence of NAD^+. Consequently, ΔligDLN was nearly completely unable to convert GGE stereoisomers (Fig. 4). These results indicated that both *ligL* and *ligN* contribute to the degradation of (α*S*,β*R*)-GGE and (α*S*,β*S*)-GGE.

Conclusions. We determined here for the first time the microbial stereospecific catabolism of four different arylglycerol-β-aryl ether stereoisomers, as shown in Fig. 5. LigD is involved in the conversion of (α*R*)-GGE, whereas LigL and LigN participate in (α*S*)-GGE transformation. Based on our previous studies (10), (β*S*)-MPHPV and (β*R*)-MPHPV were found to be the substrates for LigF and LigE, respectively. LigO has the same stereospecificity as LigD, but *ligO*'s contribution to the transformation of (α*R*)-GGE was negligible. This fact suggested that there was low expression of *ligO* at the transcriptional and/or translational level. A transcriptional analysis is necessary to confirm this hypothesis.

Interestingly, a database search revealed that orthologs of all of the β-aryl ether catabolic genes, including *ligD*, *ligL*, *ligN*, *ligE*, and *ligF* but not *ligG*, were specifically present in *N. aromaticivorans* DSM 12444 (e value range, $5e^{-57}$ to $2e^{-122}$). This suggested that DSM 12444 is a possible degrader of arylglycerol-β-aryl ether. However, the *lig* genes in DSM 12444 are widely scattered throughout the genome. It should be noted that the *ligDFEG* operon products can degrade (α*R*,β*S*)-GGE and (α*R*,β*R*)-GGE, but only (α*R*,β*S*)-GGE can be converted to β-hydroxypropiovanillone due to the lack of the GST gene involved in the elimination of glutathione from α-glutathionyl-β-hydroxypropiovanillone [GS-HPV (II) in Fig. 5]. The occurrence of a specific operon for the degradation of one of the four GGE stereoisomers in SYK-6 is intriguing. The reason for this occurrence is not clear, but the formation of this operon might be influenced by differences in the abundance of the arylglycerol-β-aryl ether stereoisomers in the environment.

ACKNOWLEDGMENT

This work was supported in part by a grant from the Ministry of Agriculture, Forestry and Fisheries of Japan (Rural Biomass Research Project BM-D1310).

REFERENCES

1. **Adler, E., and E. Eriksoo.** 1955. Guaiacylglycerol and its β-guaiacyl ether. Acta Chem. Scand. **9:**341–342.
2. **Akiyama, T., K. Magara, Y. Matsumoto, G. Meshitsuka, A. Ishizu, and K. Lundquist.** 2000. Proof of the presence of racemic forms of arylglycerol-β-aryl ether structure in lignin: studies on the stereo structure of lignin by ozonation. J. Wood Sci. **46:**414–415.
3. **Bolivar, F., and K. Backman.** 1979. Plasmids of *Escherichia coli* as cloning vector. Methods Enzymol. **68:**245–267.
4. **Bradford, M. M.** 1976. A rapid and sensitive method for the quantitation of microgram quantities of protein utilizing the principle of protein-dye binding. Anal. Biochem. **72:**248–254.
5. **Ditta, G., S. Stanfield, D. Corbin, and D. R. Helinski.** 1980. Broad host range DNA cloning system for gram-negative bacteria: construction of a gene bank of *Rhizobium meliloti*. Proc. Natl. Acad. Sci. USA **77:**7347–7351.
6. **Figurski, D. H., and D. R. Helinski.** 1979. Replication of an origin-containing derivative of plasmid RK2 dependent on a plasmid function provided in *trans*. Proc. Natl. Acad. Sci. USA **76:**1648–1652.
7. **Hosoya, S., K. Kanazawa, H. Kaneko, and J. Nakano.** 1980. Synthesis of guaiacylglycerol-β-guaiacyl ether. Mokuzai Gakkaishi **26:**118–121.
8. **Katayama, Y., S. Nishikawa, A. Murayama, M. Yamasaki, N. Morohoshi, and T. Haraguchi.** 1988. The metabolism of biphenyl structures in lignin by the soil bacterium (*Pseudomonas paucimobilis* SYK-6). FEBS Lett. **233:**129–133.
9. **Katayama, Y., S. Nishikawa, M. Nakamura, K. Yano, M. Yamasaki, N. Morohoshi, and T. Haraguchi.** 1987. Cloning and expression of *Pseudomonas paucimobilis* SYK-6 genes involved in the degradation of vanillate and protocatechuate in *P. putida*. Mokuzai Gakkaishi **33:**77–79.
10. **Masai, E., A. Ichimura, Y. Sato, K. Miyauchi, Y. Katayama, and M. Fukuda.** 2003. Roles of the enantioselective glutathione *S*-transferases in cleavage of β-aryl ether. J. Bacteriol. **185:**1768–1775.
11. **Masai, E., Y. Katayama, and M. Fukuda.** 2007. Genetic and biochemical investigations on bacterial catabolic pathways for lignin-derived aromatic compounds. Biosci. Biotechnol. Biochem. **71:**1–15.
12. **Masai, E., S. Kubota, Y. Katayama, S. Kawai, M. Yamasaki, and N. Morohoshi.** 1993. Characterization of the Cα-dehydrogenase gene involved in the cleavage of β-aryl ether by *Pseudomonas paucimobilis*. Biosci. Biotechnol. Biochem. **57:**1655–1659.
13. **Masai, E., M. Sasaki, Y. Minakawa, T. Abe, T. Sonoki, K. Miyauchi, Y. Katayama, and M. Fukuda.** 2004. A novel tetrahydrofolate-dependent *O*-demethylase gene is essential for growth of *Sphingomonas paucimobilis* SYK-6 with syringate. J. Bacteriol. **186:**2757–2765.
14. **Peng, X., T. Egashira, K. Hanashiro, E. Masai, S. Nishikawa, Y. Katayama, K. Kimbara, and M. Fukuda.** 1998. Cloning of a *Sphingomonas paucimobilis* SYK-6 gene encoding a novel oxygenase that cleaves lignin-related biphenyl and characterization of the enzyme. Appl. Environ. Microbiol. **64:**2520–2527.
15. **Reece, K. S., and G. J. Phillips.** 1995. New plasmids carrying antibiotic-resistance cassettes. Gene **165:**141–142.
16. **Reid, M. F., and C. A. Fewson.** 1994. Molecular characterization of microbial alcohol dehydrogenases. Crit. Rev. Microbiol. **20:**13–56.
17. **Schäfer, A., A. Tauch, W. Jäger, J. Kalinowski, G. Thierbach, and A. Pühler.** 1994. Small mobilizable multi-purpose cloning vectors derived from the *Escherichia coli* plasmids pK18 and pK19: selection of defined deletions in the chromosome of *Corynebacterium glutamicum*. Gene **145:**69–73.
18. **Short, J. M., J. M. Fernandez, J. A. Sorge, and W. D. Huse.** 1988. λ ZAP: a bacteriophage λ expression vector with in vivo excision properties. Nucleic Acids Res. **16:**7583–7600.
19. **Studier, F. W., and B. A. Moffatt.** 1986. Use of bacteriophage T7 RNA polymerase to direct selective high-level expression of cloned genes. J. Mol. Biol. **189:**113–130.
20. **Takeuchi, M., F. Kawai, Y. Shimada, and A. Yokota.** 1993. Taxonomic study of polyethylene glycol-utilizing bacteria: emended description of the genus *Sphingomonas* and new descriptions of *Sphingomonas macrogoltabidus* sp. nov., *Sphingomonas sanguis* sp. nov. and *Sphingomonas terrae* sp. nov. Syst. Appl. Microbiol. **16:**227–238.
21. **Yanisch-Perron, C., J. Vieira, and J. Messing.** 1985. Improved M13 phage cloning vectors and host strains: nucleotide sequences of the M13mp18 and pUC19 vectors. Gene **33:**103–119.